



Solute transport in multiple-reach experiments: Evaluation of parameters and reliability of prediction

Yan Ge, Michel C. Boufadel*

Department of Civil and Environmental Engineering, Temple University, 1947 N. 12th Street, Philadelphia, PA 19122, USA

Received 22 July 2004; revised 5 July 2005; accepted 18 August 2005

Abstract

We used two stream tracer studies to address issues related to using the transient storage model (TSM) in simulating solute transport in streams containing riffle-pools and step-pools. The injection durations were short such that one may consider the storage zones to consist mainly of surface water storage zones. We found that the TSM was not able to reproduce the high portion (near the peak) of the breakthrough curve in the first subreach (85 m) regardless of the functional form of the objective function. We attributed this to the presence of a large pool 35 m downstream of the injection location that caused segregation of solute flow that was completely mixed across the stream upstream of the pool. The model was able to closely fit the breakthrough curves at $x=185$ and 323 m, most likely because the signature of the pool diminished downstream. The fitting method did not always ensure that the parameter values represented physical reality, and we believe that physical measurements should be made and incorporated into the parameter estimation procedure utilizing Bayesian estimation. Our findings indicate that the representative values of TSM parameters in a reach do not generally fall between the representative values of its subreaches. Hence, the expression ‘reach-averaged’ should be used cautiously. The results indicated that it is more reliable to extrapolate (going downstream) than to interpolate. We believe this is due to local physical controls that could not be accounted for with parameters estimated far downstream from the controls.

© 2005 Elsevier B.V. All rights reserved.

Keywords: Dead zone; Storage area; Transient storage; Transport in streams

1. Introduction

Streams contain stagnant zones due to recirculating eddies (from meanders) and obstructions (cobbles, woody debris, etc.) to stream flow. The fraction of

stream water that enters these stagnant zones (also called dead zones) is thus temporarily retained before being released to the main channel (Thackston and Schnell, 1970; Valentine and Wood, 1977). Similarly, a fraction of stream water enters the permeable subsurface surrounding the stream (the hyporheic zone) and moves downstream at a slower velocity than that of the main channel. Eventually the water exits the hyporheic zone back to the stream. Due to

* Corresponding author. Tel.: +1 215 204 7871; fax: +1 215 204 4696.

E-mail address: boufadel@temple.edu (M.C. Boufadel).

this transverse exchange, the dead zones and the hyporheic zone act as storage zones that attenuate the peak concentration of a finite-duration input of solute to the stream, but provide slow release back to the stream after the pulse has passed (Jones and Mulholland, 2000). This slow release is manifested by a long tail in the breakthrough curves (Nordin and Troutman, 1980; Bencala and Walters, 1983; Jackman et al., 1984; Stream Solute Workshop, 1990; Runkel, 1998; Harvey and Fuller, 1998; Chapra and Runkel, 1999; Choi and Harvey, 2000; Gabriel and Boufadel, 2002).

A commonly referenced conceptual model that simulates solute transport in natural streams is the transient storage model (TSM) (Runkel, 1998). In the TSM, solute transport in the main channel is modelled using the one-dimensional advection-dispersion equation, and the transverse exchange with the storage zones is modelled using mass transfer terms. The parameters of the model are typically reach-representative due to the absence of information at the sub-reach scale. Their values are typically estimated by fitting the model to breakthrough curves obtained from stream tracer experiments.

In this paper we pose three questions associated with the TSM: (1) How much do the parameter values represent the physical reality of the stream? (2) How does one obtain a reach-representative value for a parameter if the parameter was estimated in all subreaches that constitute the reach? and (3) How reliable is the prediction?

We attempt to answer these questions using two stream-tracer experiments in a 323 m reach in Philadelphia, Pennsylvania USA.

2. Stream-tracer experiments

The study reach (Fig. 1) has a length of 323 m, and is about 4 km from the source of Indian Creek, in Fairmount Park, Philadelphia, Pennsylvania, USA. Streambed material is alluvium. The drainage area of the study reach is about 2 km², and about 50% of it is 'urban'. The reach is located in a small forest (about 200 m on each side of the reach). The top 20 cm of the streambed is a poorly sorted alluvial mixture of cobbles, gravel, sand, and sandy loam. The grain sizes range from 5 cm to less than 1 mm. Measurements of the saturated hydraulic conductivity on three cores

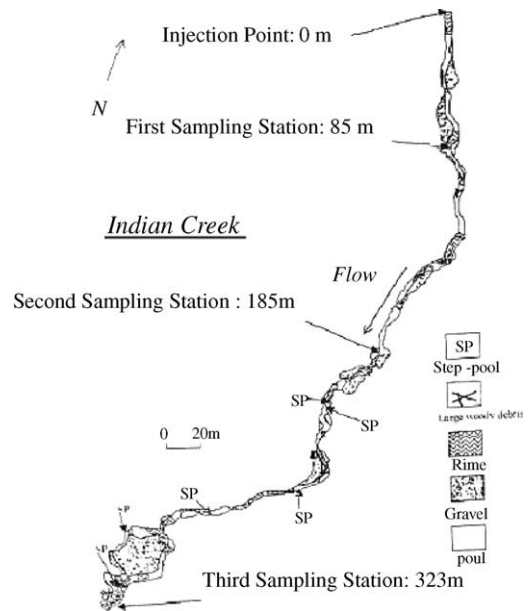


Fig. 1. Studied stream reach at Indian creek (Gabriel, 2001).

randomly extracted from the streambed gave an average value of 0.1 cm s^{-1} (Gabriel, 2001, p. 20). The lower layer is sharply finer and the bedrock is estimated to be about 2 m below the streambed. The soil of the floodplains is composed of a surficial organic horizon above a fine alluvium. The saturated hydraulic conductivity of the alluvium was measured to be $6.6 \times 10^{-5} \text{ cm s}^{-1}$ (Gabriel, 2001, p. 20). The average stream water depth (in May 2001) varied from less than 3 cm in riffles to more than 50 cm in some pools. The discharge (Q), estimated by fitting the TSM to the observed breakthrough curve (discussed in Section 6), was about $0.03 \text{ m}^3 \text{ s}^{-1}$ in May 2001. The average slope was 1.8% in Subreach 1 (0–85 m), 2.3% in Subreach 2 (85–185 m), and 4% in Subreach 3 (185–323 m).

The stream varies from riffle-pools in Subreach 1 to step-pool in Subreach 3. The sinuosity of the stream increases going from Subreach 1 to Subreach 3, which has alternating meanders with wavelengths of 10–20 m.

Two stream tracer experiments were conducted using sodium chloride (NaCl) as a conservative tracer. The concentration of salt in the injection tank was measured to be 54 g L^{-1} in Experiment 1

and 50 g L^{-1} in Experiment 2. The injection durations were 37 and 81 min, respectively. The flow rate of injection was approximately 1.0 L s^{-1} , and it was applied to the stream through a manifold that was placed across the stream to maximize transverse mixing. Grab samples of 100 ml were obtained at 85, 185, and 323 m, by dipping 120 ml polystyrene containers in the stream. The sampling intervals were 2 and 3 min, for Experiment 1 and Experiment 2, respectively. Salt concentrations were monitored using calibrated electrical conductivity (EC) measurements. Figs. 2 and 3 report the observed breakthrough curves (symbols represent measured data and lines represent model output). The background concentration of salts was about 240 mg L^{-1} in both experiments. The peak values ranged from 850 to about 1200 mg L^{-1} . This made it plausible to utilize electrical conductivity as a surrogate measure for the amount of salt in water, and the errors in EC readings that result from different hydration properties of various salts could be considered negligible. All of the breakthrough curves reveal the sudden rise and slow fall observed in other tracer studies (Bencala and Walters, 1983; Harvey et al., 1996).

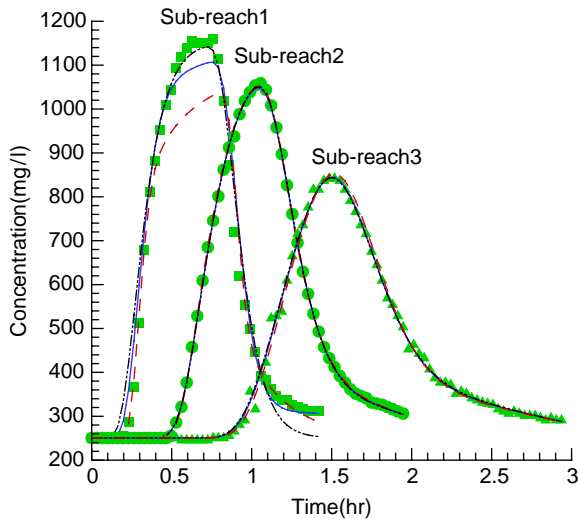


Fig. 2. Fitting curve of Subreach 1, Subreach 2, and Subreach 3 (Experiment 1) (solid curve is $m=0$, dashed curve is $m=2$, dash-dot curve is $m=-1$).

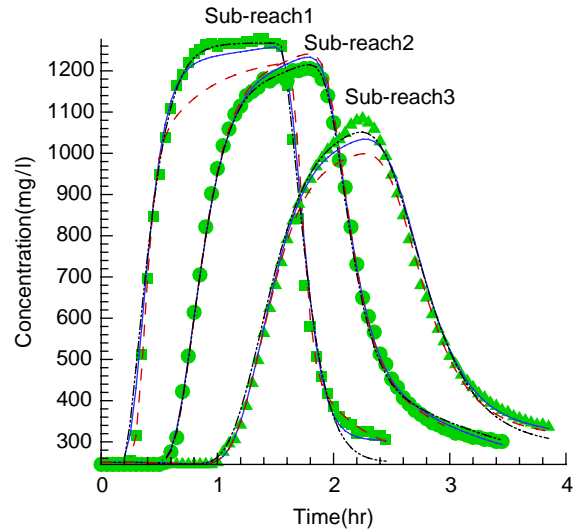


Fig. 3. Fitting curve of Subreach 1, Subreach 2, and Subreach 3 (Experiment 2) (solid curve is $m=0$, dashed curve is $m=2$, dash-dot curve is $m=-1$).

3. Simulation procedure

The governing equations for the TSM are (Bencala and Walters, 1983; Runkel, 1998):

$$A \frac{\partial C}{\partial t} = -Q \frac{\partial C}{\partial x} + \frac{\partial}{\partial x} \left(AD \frac{\partial C}{\partial x} \right) + q_{\text{lin}}(C_1 - C) + \alpha A(C_s - C) \quad (1)$$

$$A_s \frac{dC_s}{dt} = \alpha A(C - C_s) \quad (2)$$

Where, C [mg L^{-1}] is the concentration in the stream, C_s [mg L^{-1}] is the concentration in the storage zone, C_1 [mg L^{-1}] is the concentration of the transverse groundwater flow, A [m^2] is the main channel cross sectional area, A_s [m^2] is the cross sectional area of the storage zone, D [$\text{m}^2 \text{ s}^{-1}$] is the dispersion coefficient, Q [$\text{m}^3 \text{ s}^{-1}$] is the volumetric flow rate, q_1 [$\text{m}^3 \text{ s}^{-1} \text{ m}^{-1}$] is the lateral flow rate coming into the stream (positive) per unit stream length, t [s] is time, α [s^{-1}] is a storage zone exchange coefficient, and x [m] is the along stream distance from the injection location. All dependent variables in Eqs. (1) and (2) could vary with x . Eq. (1) simulates the transport in the main channel by advection (the first term on the right hand

side) and dispersion (the second term). The third term represents the incoming mass directly from the groundwater, which is assumed to bypass the storage zones and enter directly into the main channel. The last term represents the exchange of solute with the storage zones. Eq. (2) represents conservation of mass in the storage zone. The right hand side of Eq. (2) represents the exchange flux with the main channel. The sign of this term is opposite that of the last term in Eq. (1). Implicit in Eq. (1) is the conservation of mass of water given by the equation:

$$\frac{dQ}{dx} = q_{\text{lin}} - q_{\text{lout}} \quad (3)$$

Where, q_{lout} [$\text{m}^3 \text{s}^{-1} \text{m}^{-1}$] is the lateral outflow per unit stream length, taken positive if water leaves the stream and zero otherwise.

4. The direct problem

The direct problem consists of solving Eqs. (1) and (2) for known parameters and initial and boundary conditions. In this work, Eq. (1) was discretized using the Crank–Nicolson method, which is second order accurate in both time and space. The advection term in Eq. (1) was discretized using central differencing, which is a second order scheme in space. This numerical approach is the same approach used in the USGS model, OTIS (Runkel, 1998). Eqs. (1) and (2) were solved with the following conditions:

Initial conditions, IC:

$$C(x, t = 0) = C_s(x, t = 0) = C_{\text{lin}}(x, t = 0) = C_b \quad (4)$$

Where C_b is the background concentration.

Boundary conditions, BC:

$$x = 0, \quad t \leq t_{\text{injection}} :$$

$$C = \frac{(C_b \times Q_0 + C_{\text{inj}} \times q_{\text{inj}})}{(Q_0 + q_{\text{inj}})} \quad (5a)$$

$$x = 0, \quad t > t_{\text{injection}} : \quad C = C_b \quad (5b)$$

$$x = L : \quad \frac{\partial C}{\partial x} = 0 \quad (5c)$$

Where, Q_0 is discharge at $x=0$, C_{inj} [mg L^{-1}] is the injection concentration, q_{inj} [$\text{m}^3 \text{s}^{-1}$] is the injection flow rate, and L is the total length of subreach (or

reach) being modelled. Eq. (5c) represents an ‘out-flowing’ boundary condition, where advection is the only mechanism to carry the solute out of the subreach or reach that is being modelled.

5. Parameter estimation

Six parameters were estimated. They are D , A , Q , q_1 , α , and A_s . These parameters were estimated by inverse modeling (as opposed to the direct problem) by minimizing the residuals between the simulated and observed results. A general weighted least square objective function was used:

$$F = \sum_{i=1}^N \frac{(C_i - C_{o,i})^2}{(C_{o,i})^m} \quad (6)$$

Where, $C_{o,t}$ represents the observed concentration at time $t=i\Delta t$ (Figs. 1 and 2), C_i is the simulated concentration, and N is number of observed values in fitting to each breakthrough curve. The index ‘ t ’ corresponds to time $t=i\Delta t$, where i is the sample number and Δt is the sampling interval (2 min for Experiment 1 and 3 min for Experiment 2). The term m takes three values: -1 , 0 and 2 . Its value is intended to give more emphasis on fitting a certain portion of the breakthrough curve. A value of $m=-1$ results in higher emphasis on matching the high values, namely the peak value. Such a weight is used in the US Army Corps of Engineer program for rainfall-runoff modeling, HEC-HMS (HEC-HMS, 2001, p. 130–131). A value of $m=2$ gives more emphasis on matching the low values, and in particular the tail of the breakthrough curve. The value $m=0$ results in the ordinary least square, and it is an intermediate case. This case has the advantage that it provides parameter estimates that are statistically unbiased (Bard, 1974; Beck and Arnold, 1977; Boufadel, 1998).

The minimization algorithm used in this study is a generalized reduced gradient technique called GRG2 (Lasdon et al., 1979). Lower and upper bounds on decision variables are quite easy to handle with GRG2. The GRG2 requires a user-supplied subroutine GCOMP to compute the objective function and the constraints for values of the decision variables. Supplementary information on the software can be found in Lasdon and Warren (1980), and applications of GRG2 in hydrology can be found elsewhere (Unver

and Mays, 1984; Boufadel, 1998; Boufadel et al., 1998).

6. Results

6.1. Validity of the one-dimensional transport assumption

Each subreach was fitted separately. The boundary conditions given by Eq. (5) were used for Subreach 1. For the remaining subreaches, the observed breakthrough concentration at the beginning of the subreach was used as input to the model, and the background concentration was used as input after the last observed measurement. Because the model uses a time step that is smaller than that used for measurement, the concentration values were linearly interpolated between measured values. The flow rate at the beginning of each subreach was estimated by the fitting procedure. The outflowing boundary condition was used at the end of each subreach. The initial conditions were those presented in Eq. (4).

Fig. 2 shows the fitted curve to the data from Experiment 1. The fit was very good for Subreach 2 and Subreach 3, and the 'm' value did not seem to make a difference. The fit to Subreach 1 was poor for all m values. Fig. 3 shows that the fitted curve to Subreach 2 and Subreach 3 in Experiment 2 is not as good as in Experiment 1, but different 'm' values were able to well represent various portions of the breakthrough curve. This is further discussed in Section 6.2.

The poor fit to Subreach 1 is most likely due to two-dimensional transport that could not be simulated by the one-dimensional equations (Eqs. (1) and (2)), which assume that the solute is completely mixed in the transverse direction of the stream. We believe that the transport was initially one-dimensional in the stream due to the fact that we used a manifold to inject the tracer across the stream. However, at about $x = 35$ m, a large pool was present; the cross sectional area in the mid-section of the pool was about 1.8 m^2 , while it was less than 0.5 m^2 before and after the pool (Gabriel, 2001, p. 25). The solute that entered the pool was (most likely) completely mixed in the transverse direction, but water flow in the pool was essentially two-dimensional, with higher velocities along the center of the pool and lower velocities near the edge.

This probably caused segregation of the flow, a typical problem in chemical reactors with low mixing (Levenspiel, 1999, p. 257). For downstream transport, solute behaved as if it was emanating from a point source (the center line of the pool), and the short distance of Subreach 1 past the pool (a mere 40 m) did not provide enough time for mixing of the tracer across the stream sections.

Rutherford (1994, p. 123) developed a criterion for the minimum stream length necessary for complete mixing in the cross section of a stream if the tracer were injected in the midsection of the stream (point injection). The criterion was further discussed by Harvey et al. (1996), and it is:

$$L_c = \beta \left(\frac{ub^2}{k_z} \right) \quad (7)$$

where L_c is the minimum distance for complete mixing, u is the average velocity of the stream, and b is the width of the stream. For our case, $b = 3$ m and $d = 0.1$ m, d is the channel depth. The parameter k_z is the transverse dispersion coefficient and can be estimated as $0.4du^*$ (Rutherford, 1994, p. 109), where u^* is the shear velocity. Rutherford (1994, p. 123) reports a value for β of 0.134 for a mid channel source. The shear velocity, u^* , is usually larger than $u/25$ (Rutherford, 1994, p. 70), so one could adopt the value $u^* = 0.1u$.

$$L_c = 0.134 \left(\frac{9}{0.24 \times 0.1 \times 0.1} \right) = 502.5 \text{ m} \quad (8)$$

This value is apparently too large because the one-dimensional model (Eqs. (1) and (2)) was able to closely fit the observed breakthrough curves at shorter distances ($x = 185$ and 323 m). The criterion given by Eq. (7) was obtained based on studies in (large) rivers and gradually varying irrigation channels, where it was assumed that the water flow is affected predominantly by streambed roughness (i.e. Manning's roughness). However, a recent study by Lane et al. (2004) indicates that local streambed topography plays a major role in controlling water flow in comparison with small-scale surface roughness. Hence, the shear velocity in the reach used in this study is most likely much larger than estimated by Rutherford (1994), which would result in an L_c value that is smaller than that given by Eq. (7).

Our results thus show that the one-dimensional representation was capable of simulating the transport occurring in Subreaches 2 and 3, but not in Subreach 1. For this reason, the parameter values of Subreach 1 will not be further discussed.

6.2. How much do the parameters reflect the physical reality?

Different ‘m’ values improved the fit of the model output to different portions of the observed breakthrough curve. As shown in Figs. 2 and 3, a value of $m=2$ allowed a better fit to the tail of the breakthrough curve while a value of $m=-1$ allowed a better fit to the peak of the breakthrough curve, but the fit to the tail was very poor, as shown in Figs. 2 and 3. For this reason, we favor the value $m=0$ over $m=-1$ in matching the peak

Each parameter or set of parameters affects a certain region of the breakthrough curve. This fact was discussed in Stream Solute Workshop (1990), and

was thoroughly analyzed by Harvey and Fuller (1998), who conducted sensitivity analysis of the breakthrough curve based on Monte Carlo simulations. In summary, the high values of the breakthrough curve are sensitive to Q , A , D , and q_1 . This probably explains the effectiveness of the advection dispersion equation without transverse exchange to accurately simulate the peaks in early studies. Fisher (1979, p. 132) suggested ignoring the tail of the observed breakthrough curve when using the advection-dispersion equation without transverse exchange. The tail of the breakthrough curve is more sensitive to the transient storage parameters (α , A_s). Hence, $m=0$ provide good estimates of Q , A , D , and q_1 , while $m=2$ provides good estimates of α and A_s . The values of q_1 might be less physically based in this work due to the absence of groundwater flow information. They are reported herein only for completeness.

The dispersion coefficient in Subreach 2 estimated by $m=0$ was essentially the same in both experiments (Table 1). The dispersion coefficient in Subreach 3

Table 1
Fitting result for three Subreaches

Subreaches	Experiment 1			Experiment 2		
	$m=-1$	$m=0$	$m=2$	$m=-1$	$m=0$	$m=2$
Dispersion coefficient, D , ($m^2 s^{-1}$)						
Subreach 1	3.38×10^{-01}	2.29×10^{-01}	8.73×10^{-02}	3.28×10^{-02}	2.43×10^{-01}	8.23×10^{-02}
Subreach 2	2.44×10^{-01}	2.40×10^{-01}	1.60×10^{-01}	2.30×10^{-01}	2.43×10^{-01}	1.98×10^{-01}
Subreach 3	5.56×10^{-01}	5.19×10^{-01}	4.38×10^{-01}	5.23×10^{-01}	3.35×10^{-01}	3.26×10^{-01}
Upstream flow rate, Q ($m^3 s^{-1}$)						
Subreach 1	5.87×10^{-02}	3.78×10^{-02}	6.38×10^{-02}	4.79×10^{-02}	3.21×10^{-02}	4.95×10^{-02}
Subreach 2	1.60×10^{-02}	1.99×10^{-02}	2.58×10^{-02}	4.91×10^{-02}	5.90×10^{-02}	6.54×10^{-02}
Subreach 3	1.97×10^{-01}	1.25×10^{-01}	1.02×10^{-01}	9.44×10^{-02}	7.82×10^{-02}	3.80×10^{-02}
Storage coefficient, α , (s^{-1})						
Subreach 1	7.71×10^{-04}	3.96×10^{-04}	3.39×10^{-04}	3.67×10^{-03}	2.53×10^{-04}	2.06×10^{-04}
Subreach 2	1.77×10^{-04}	1.93×10^{-04}	3.72×10^{-04}	1.21×10^{-04}	1.53×10^{-04}	1.66×10^{-04}
Subreach 3	9.86×10^{-05}	9.98×10^{-05}	9.59×10^{-05}	6.70×10^{-05}	9.64×10^{-05}	1.18×10^{-04}
Lateral flow rate, q_L , ($m^2 s^{-1}$)						
Subreach 1	-6.46×10^{-06}	2.80×10^{-05}	2.40×10^{-07}	-2.33×10^{-05}	2.29×10^{-05}	-5.06×10^{-06}
Subreach 2	7.12×10^{-06}	8.76×10^{-06}	1.00×10^{-05}	-1.90×10^{-07}	6.73×10^{-06}	-9.52×10^{-07}
Subreach 3	3.30×10^{-07}	2.95×10^{-07}	3.21×10^{-07}	4.00×10^{-06}	-1.75×10^{-06}	-2.63×10^{-06}
Main channel area, A , (m^2)						
Subreach 1	8.03×10^{-01}	5.93×10^{-01}	8.56×10^{-01}	4.73×10^{-01}	6.56×10^{-01}	8.39×10^{-01}
Subreach 2	2.22×10^{-01}	2.75×10^{-01}	3.30×10^{-01}	7.71×10^{-01}	9.17×10^{-01}	9.99×10^{-01}
Subreach 3	$2.76E+00$	$1.75E+00$	$1.44E+00$	$1.62E+00$	$1.27E+00$	6.16×10^{-01}
Storage area, A_s , (m^2)						
Subreach 1	9.43×10^{-02}	$2.96E+00$	2.29×10^{-01}	4.11×10^{-01}	$4.97E+00$	4.11×10^{-01}
Subreach 2	2.24×10^{-02}	3.12×10^{-02}	5.95×10^{-02}	2.34×10^{-01}	2.19×10^{-01}	2.22×10^{-01}
Subreach 3	$1.49E+00$	$1.03E+00$	9.12×10^{-01}	$1.80E+01$	$2.32E+00$	$2.00E+00$

estimated in Experiment 2 was about 65% of the value estimated in Experiment 1. The dispersion coefficient in Subreach 2 was smaller than that in Subreach 3, and is most likely due to the presence of many large pools (about 1.0 m deep) in Subreach 3; pools have large longitudinal dispersion coefficients because the transverse mixing in them is relatively weak in comparison with riffles.

The cross sectional area ($m=0$) in Subreach 2 was smaller in Experiment 1 than in Experiment 2. The opposite was noted in Subreach 3, which is unexpected, because the water level in Experiment 2 was higher than in Experiment 1. The cross sectional area of Subreach 2 was smaller than that of Subreach 3, in both experiments (Table 1). This is expected due to the presence of large pools in Subreach 3.

In Subreach 2, the transient storage exchange coefficient, α ($m=2$), increased by a factor of two between Experiment 1 and Experiment 2. In Subreach 3, α increased by only about 20% between Experiment 1 and Experiment 2. The large value of α in Subreach 2 with respect to Subreach 3 is logical, because Subreach 2 is made mostly of riffle-pools while Subreach 3 is made of step-pools. The flow in riffles occurs usually over gravelly streambeds, which enhances the exchange between the main channel and storage zones around and below the gravel.

The transient storage area, A_s ($m=2$), in Subreach 3 was larger than the transient storage area in Subreach 2 in both experiments. This was most likely due to the presence of pools in Subreach 3. Portions of these pools away from the thalweg probably behaved as dead zones. The A_s values in both Subreach 2 and Subreach 3 were larger in Experiment 2 than in Experiment 1. This can be explained by the fact that in Experiment 2 the stream was losing water to the subsurface, as shown by the negative q_1 values of Experiment 2 (Table 1).

For Subreach 3, the estimated flow rate ($m=0$) in Experiment 1 was larger than that estimated in Experiment 2. This was unexpected because the water level at the riffle below the injection manifold in Experiment 2 was higher by about 3 cm than in Experiment 1. We considered and ruled out many physically based possibilities for this unexpected result. But we are hesitant to claim that using a stream-tracer experiment does not allow accurate

estimation of the discharge, because such an approach has been used for the previous four decades to gauge streams (Thackston and Schnell, 1970; Bencala and Walters, 1983). It is possible that the minimization algorithm found a local optimum.

6.3. The representative values of a subreach

Due to the lack of detailed physical information about most reaches, the parameters of the transient storage model (Eqs. (1) and (2)) are considered ‘reach-averages’. However, the term average is in fact a misnomer, and it is preferable to use the term ‘reach-representative’ unless one can ascertain that the values represent some kind of an average of the values estimated at smaller scales. We attempt to address this issue by considering portions of the stream whose subreach values are known.

We considered Subreach 23, which is the stream portion starting at $x=85$ m and ending at $x=323$ m. This subreach is thus made up of Subreach 2 and Subreach 3. The parameter values of Subreach 23 were estimated by fitting the TSM to the breakthrough curve at $x=323$ m using the breakthrough curve at 85 m as input to the model. We also considered Subreach 123 (0–323 m, i.e. the whole reach), and we viewed it as made up of Subreach 12 (0–185 m) and Subreach 3. Figs. 4–7 report the values of four parameters (D , α , A , and A_s) obtained for $m=0$. The standard deviations of these values were computed according to the procedure explained below. The exact values of the parameters and their standard deviations are reported in Tables 2 and 3.

The standard deviation of estimates can be computed as (Bard, 1974, p178):

$$\sigma_{\theta}^2 = \sigma_c^2 \left(\frac{\partial^2 F_o}{\partial \theta^2} \right)^{-1} \quad (9)$$

where θ represents any of the parameters, and the term in parentheses represents the diagonal terms of the Hessian matrix (evaluated at the optimum). F_o is the objective function at the optimum ($F_o = \sum_{i=1}^n (C_{i,o} - C_i)^2$). The quantity is the standard error (standard deviation of the residuals) given by:

$$\sigma_c^2 = \frac{F_o}{n-p} \quad (10)$$

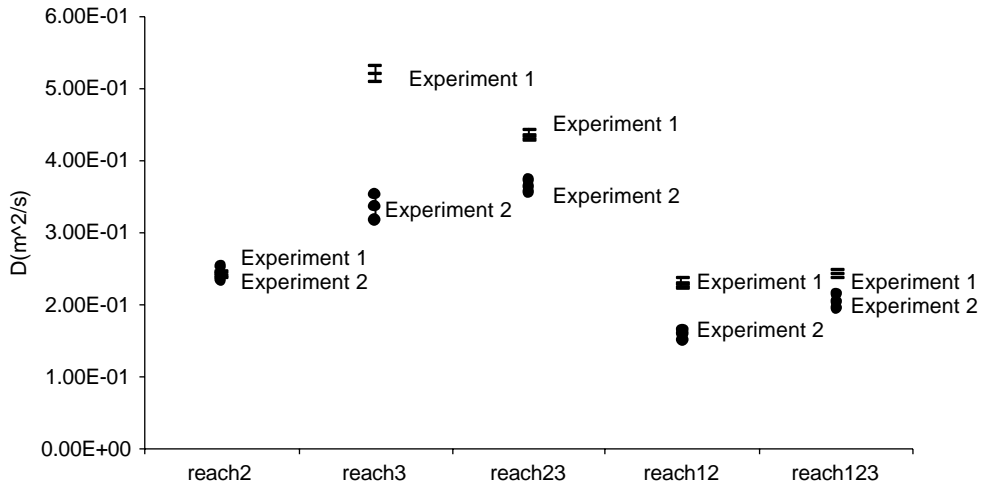


Fig. 4. Estimation of D .

where, n is the number of observed data points ($n=60$ for Subreach 2, $n=90$ for Subreach 3 in Experiment 1, and $n=70$ for Subreach 2, $n=78$ for Subreach 3 in Experiment 2, respectively.), and p is the number of parameters to be estimated ($p=6$).

Eq. (9) is obtained assuming the model is linear and the residuals are normally distributed (Beck and Arnold, 1977; Bard, 1974). However, our model (Eqs. (1) and (2)) is non-linear, and verifying the normality of the residuals and the ensuing correcting action is outside the scope of this work. Readers interested in

such a topic are referred to the works of Kuczera (1990); Bates and Townley (1988), and Boufadel (2000). However, Eq. (9) remains useful, because it states that the uncertainty in a parameter depends on the standard deviation of the errors, σ_e (i.e. goodness of fit), and the sensitivity of the objective function to variation in the parameter (the second derivative term), which is intuitive.

The second derivative terms were evaluated numerically by varying each parameter by 5% and evaluating the objective function:

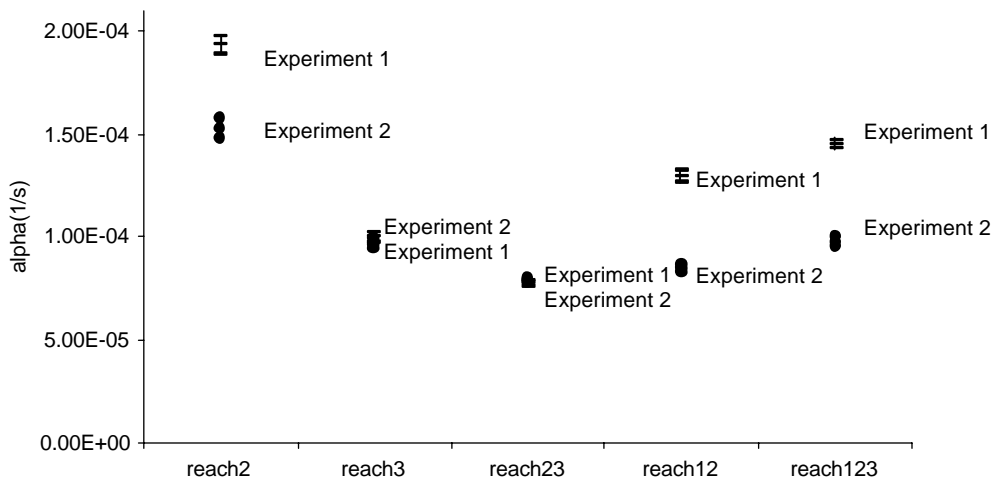


Fig. 5. Estimation of α .

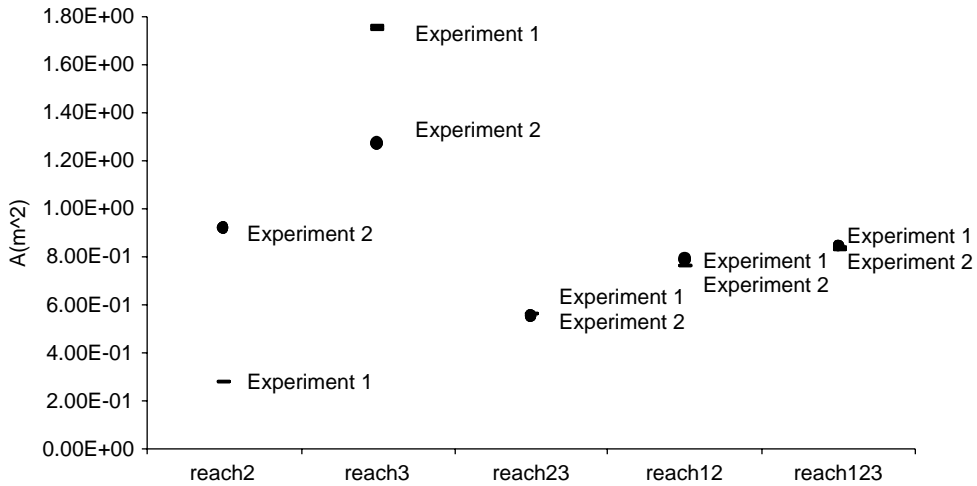


Fig. 6. Estimation of A.

$$\frac{\partial^2 F_o}{\partial \theta^2} = \frac{F(\theta + \Delta\theta) - 2F_o(\theta) + F(\theta - \Delta\theta)}{(\Delta\theta)^2} \quad (11)$$

Other studies (e.g. Gooseff et al., 2005) used smaller increments (1% of the parameter value) when numerically evaluating the sensitivity coefficients in their TSM study. Although a smaller increment makes the derivative more accurate mathematically, our selection of 5% is motivated by two reasons. The first is that the objective function is a non-linear function in the parameters' space, hence, a too small an

increment results in too localized information that might not reflect the overall trend of the objective function. The second reason is rather practical; this study supports using direct measurement to better estimate parameters, and a 1% change in a parameter is too small to be accurately measured. We believe that parameters estimated within 5–10% are accurate enough considering the variability in stream systems. For example, a stream cross section area of 1.00 m² is not, from a practical point of view, different from 1.01 m².

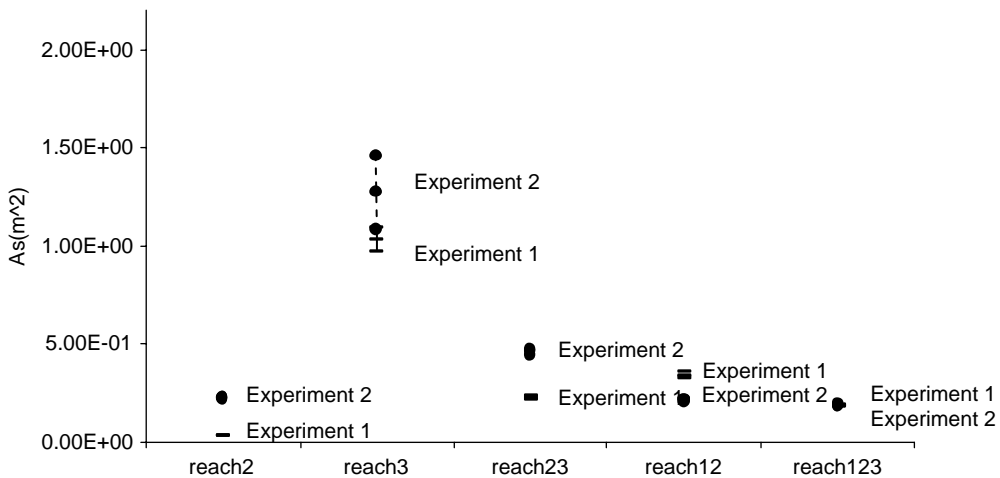


Fig. 7. Estimation of A_s.

Table 2
Fitting result for Subreach 2, Subreach 3, and Subreach 23

	Subreach 2	Subreach 3	Subreach 23
Experiment 1			
<i>D</i>	$2.40 \times 10^{-1} \pm 3.39 \times 10^{-3}$	$5.19 \times 10^{-1} \pm 1.11 \times 10^{-2}$	$4.34 \times 10^{-1} \pm 6.89 \times 10^{-3}$
<i>Q</i>	$1.99 \times 10^{-2} \pm 2.31 \times 10^{-5}$	$1.25 \times 10^{-1} \pm 3.86 \times 10^{-4}$	$4.02 \times 10^{-2} \pm 6.87 \times 10^{-5}$
<i>A</i>	$1.93 \times 10^{-4} \pm 4.43 \times 10^{-6}$	$9.98 \times 10^{-5} \pm 2.42 \times 10^{-6}$	$7.73 \times 10^{-5} \pm 1.49 \times 10^{-6}$
<i>q_l</i>	$8.76 \times 10^{-6} \pm 1.63 \times 10^{-7}$	$2.95 \times 10^{-7} \pm 9.17 \times 10^{-6}$	$2.44 \times 10^{-6} \pm 4.47 \times 10^{-7}$
<i>A</i>	$2.75 \times 10^{-1} \pm 3.21 \times 10^{-4}$	$1.75 \times 10^{00} \pm 4.97 \times 10^{-3}$	$5.61 \times 10^{-1} \pm 9.36 \times 10^{-4}$
<i>A_s</i>	$3.12 \times 10^{-2} \pm 4.13 \times 10^{-4}$	$1.03 \times 10^{00} \pm 6.02 \times 10^{-2}$	$2.22 \times 10^{-1} \pm 9.58 \times 10^{-3}$
Experiment 2			
<i>D</i>	$2.43 \times 10^{-1} \pm 9.78 \times 10^{-3}$	$3.35 \times 10^{-1} \pm 8.72 \times 10^{-2}$	$3.64 \times 10^{-1} \pm 9.12 \times 10^{-3}$
<i>Q</i>	$5.90 \times 10^{-2} \pm 1.85 \times 10^{-4}$	$7.82 \times 10^{-2} \pm 3.70 \times 10^{-4}$	$3.4 \times 10^{-2} \pm 6.74 \times 10^{-5}$
<i>A</i>	$1.53 \times 10^{-4} \pm 4.76 \times 10^{-6}$	$9.64 \times 10^{-5} \pm 2.31 \times 10^{-6}$	$7.89 \times 10^{-5} \pm 1.09 \times 10^{-6}$
<i>q_l</i>	$6.73 \times 10^{-6} \pm 1.25 \times 10^{-6}$	$1.75 \times 10^{-6} \pm 6.41 \times 10^{-6}$	-9.88×10^{-07a}
<i>A</i>	$9.17 \times 10^{-1} \pm 2.94 \times 10^{-3}$	$1.27 \times 10^{00} \pm 6.26 \times 10^{-3}$	$5.47 \times 10^{-1} \pm 1.08 \times 10^{-3}$
<i>A_s</i>	$2.19 \times 10^{-1} \pm 5.98 \times 10^{-3}$	$1.27 \times 10^{-00} \pm 1.89 \times 10^{-1}$	$4.57 \times 10^{-1} \pm 1.46 \times 10^{-2}$

^a The curvature is negative because a saddle point was encountered.

The fit to the breakthrough curves was essentially similar to that observed in Figs. 2 and 3. For this reason, the simulated breakthrough curves are not reported for brevity.

Figs. 4–7 show that the standard deviations of most parameters were relatively small, indicating that these parameters are well-determined. The figures also show that the reach-representative values of the parameters do not generally fall between those of the corresponding subreaches; they are actually many standard deviations away from the subreach values.

Hence, these values cannot be considered as average values of the subreaches' values.

The fact that the parameters' intervals did not overlap in most cases indicates that these values are inherently different. This is a situation known as 'statistical incompatibility', and is encountered, for example, in rainfall-runoff models where different storms result in different sets of parameter values that are theoretically storm-independent (Bates and Townley, 1988; Kuczera, 1990; Boufadel, 2000). This is usually due to the fact that the model is non-linear in

Table 3
Fitting result for Subreach 12, Subreach 3, and Subreach 123

	Subreach 12	Subreach 3	Subreach 123
Experiment 1			
<i>D</i>	$2.29 \times 10^{-1} \pm 7.21 \times 10^{-3}$	$5.19 \times 10^{-1} \pm 1.11 \times 10^{-2}$	$2.41 \times 10^{-1} \pm 5.54 \times 10^{-3}$
<i>Q</i>	$5.35 \times 10^{-2} \pm 1.21 \times 10^{-4}$	$1.25 \times 10^{-1} \pm 3.86 \times 10^{-4}$	$6.31 \times 10^{-2} \pm 7.73 \times 10^{-5}$
<i>A</i>	$1.29 \times 10^{-4} \pm 3.00 \times 10^{-6}$	$9.98 \times 10^{-5} \pm 2.42 \times 10^{-6}$	$1.45 \times 10^{-4} \pm 2.16 \times 10^{-6}$
<i>q_l</i>	$5.39 \times 10^{-7} \pm 1.06 \times 10^{-6}$	$2.95 \times 10^{-7} \pm 9.17 \times 10^{-6}$	$1.25 \times 10^{-7} \pm 4.09 \times 10^{-7}$
<i>A</i>	$7.56 \times 10^{-1} \pm 1.72 \times 10^{-3}$	$1.75 \times 10^{00} \pm 4.97 \times 10^{-3}$	$8.29 \times 10^{-1} \pm 1.05 \times 10^{-3}$
<i>A_s</i>	$3.37 \times 10^{-1} \pm 1.47 \times 10^{-2}$	$1.03 \times 10^{00} \pm 6.02 \times 10^{-2}$	$1.83 \times 10^{-1} \pm 3.07 \times 10^{-3}$
Experiment 2			
<i>D</i>	$1.57 \times 10^{-1} \pm 6.92 \times 10^{-3}$	$3.35 \times 10^{-1} \pm 8.72 \times 10^{-2}$	$2.04 \times 10^{-1} \pm 1.08 \times 10^{-2}$
<i>Q</i>	$4.62 \times 10^{-2} \pm 9.21 \times 10^{-5}$	$7.82 \times 10^{-2} \pm 3.70 \times 10^{-4}$	$5.40 \times 10^{-2} \pm 1.39 \times 10^{-4}$
<i>A</i>	$8.45 \times 10^{-5} \pm 2.02 \times 10^{-6}$	$9.64 \times 10^{-5} \pm 2.31 \times 10^{-6}$	$9.77 \times 10^{-5} \pm 2.89 \times 10^{-6}$
<i>q_L</i>	$5.03 \times 10^{-7} \pm 6.68 \times 10^{-7}$	$1.75 \times 10^{-6} \pm 6.41 \times 10^{-6}$	-1.67×10^{-09a}
<i>A</i>	$7.86 \times 10^{-1} \pm 1.79 \times 10^{-3}$	$1.27 \times 10^{00} \pm 6.26 \times 10^{-3}$	$8.42 \times 10^{-1} \pm 2.32 \times 10^{-3}$
<i>A_s</i>	$2.09 \times 10^{-1} \pm 7.37 \times 10^{-3}$	$1.27 \times 10^{00} \pm 1.89 \times 10^{-1}$	$1.86E - 16.54E - 3$

^a The curvature is negative because a saddle point was encountered.

the parameters of interest, as is the case herein (Eqs. (1) and (2)).

To further evaluate the physicality of the parameters, we computed the Damkohler number for each subreach, via:

$$DaI = \frac{\alpha \left(1 + \frac{A}{A_s}\right) L}{\frac{Q}{A}} \quad (12)$$

The DaI is a dimensionless number that expresses the ratio of transport in and out of the storage zones to convection. A subreach with a Damkohler number that is too small (i.e. $DaI \ll 1$) or too large ($DaI \gg 1$) indicates that the storage exchange parameters are not well represented in the breakthrough curve. A small DaI implies that very little tracer has interacted with the dead zones, whereas a large DaI implies that storage processes become dominant and they cannot be conceptually separated from mixing processes due to shear dispersion. The reader is referred to Harvey and Wagner (2000, p. 28–32) for a thorough discussion on the Damkohler number.

Application of the Eq. (12) to the mean parameter values in Tables 2 and 3 gave a Damkohler number that varied between 0.43 (for Subreach 3, Experiment 2) to 3.37 (Subreach 123, Experiment 1). The closeness of these values to 1.0 indicates that the storage exchange parameters (i.e. A , A_s , and α) are well represented in the breakthrough curve, and subsequently in the estimation procedure.

6.4. Ability to predict

A final task in our study is to evaluate the ability of the conceptual model to predict the concentration at locations where no fitting was conducted. Noting that the parameter values of subreaches are statistically different (Section 6.3), the only utility of such an approach is expedience.

Two subreaches were considered, Subreach 12 (0–185 m) and Subreach 123 (0–323 m). Recall that Subreach 12 is in Subreach 123. Figs. 8 and 9 report simulation results at $x=323$ m using the parameter values estimated at the end of Subreach 12. The value $m=0$ gave the best fit and is thus reported. One can consider that the predictive ability of this set of parameter values is good in both experiments

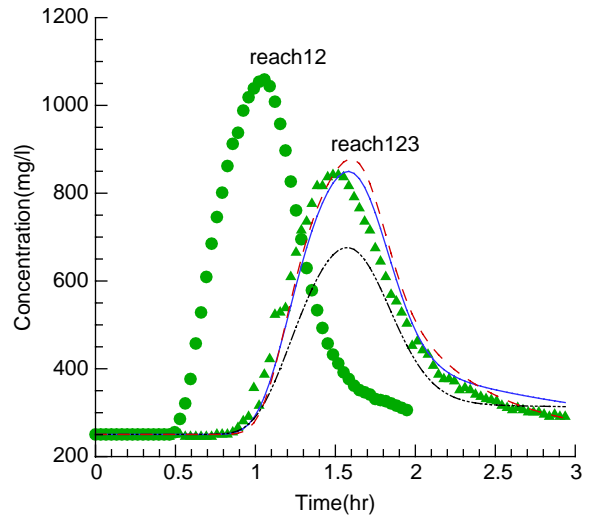


Fig. 8. Using reach 12 to Predict reach 123 (Experiment 1) (solid curve is $m=0$, dashed curve is $m=2$, dash-dot-dot curve is $m=-1$)

(although the values were different between experiments).

Figs. 10 and 11 report simulation results at $x=185$ m using the parameter values estimated at the end of Subreach 123 (i.e. the whole reach). The predictive ability is not as good as observed in Figs. 8 and 9. The value $m=-1$ provided the best fit for Experiment 2,

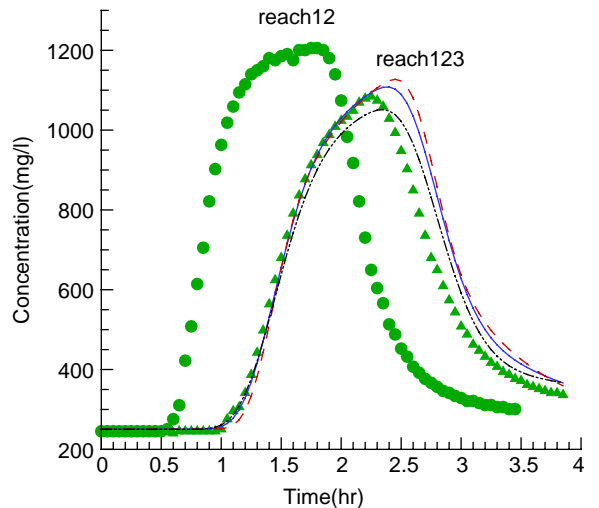


Fig. 9. Using reach 12 to Predict reach 123 (Experiment 2) (solid curve is $m=0$, dashed curve is $m=2$, dash-dot-dot curve is $m=-1$)

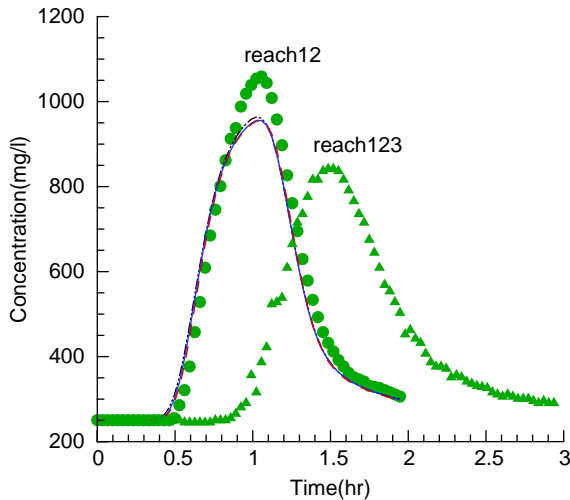


Fig. 10. Using reach 123 to Predict reach 12 (Experiment 1) (solid curve is $m=0$, dashed curve is $m=2$, dash-dot-dot curve is $m=-1$).

nonetheless the fit is only mediocre. Hence, one may conclude from Figs. 8–11 that it is better to extrapolate results than to interpolate. Although this could be viewed as counterintuitive, one should note that the identifiability of parameters decreases going away from the injection location, as noted in prior stream tracer studies (Harvey et al., 1996).

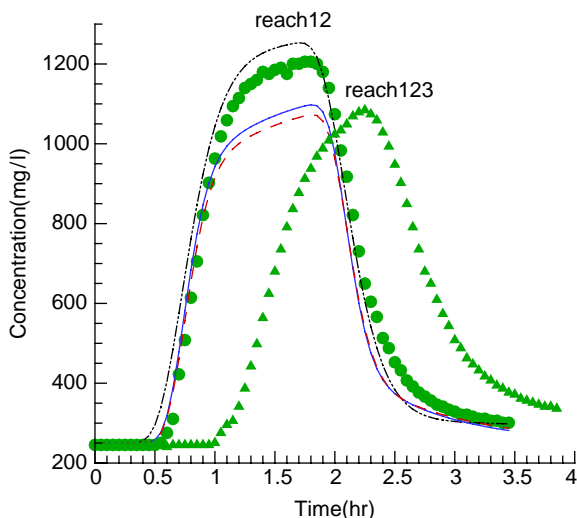


Fig. 11. Using reach 123 to Predict reach 12 (Experiment 2) (solid curve is $m=0$, dashed curve is $m=2$, dash-dot-dot curve is $m=-1$).

The situation of non-identifiability results when many combinations of parameters result in essentially the same fit (Beck and Arnold, 1977).

7. Conclusions

We used two stream tracer studies to address issues related to using the transient storage model (TSM) in simulating solute transport in streams. The experiments were conducted in a reach that contains riffle-pools and step-pools. The injection occurred through a manifold placed across the stream. The injection durations were short such that one may consider the storage zones to consist mainly of surface water storage zones (i.e. the hyporheic zone was very small). Three types of objective functions were utilized to fit the TSM to the data: The weighted least square (WLS), the ordinary least square (OLS), and an empirical type used in fitting hydrographs in rainfall-runoff studies. This last type results in a better fit near the peak of the breakthrough curve. The WLS results in a better fit of the tail of the breakthrough curve, and the OLS is an intermediate case between the two.

We found that the TSM was not able to reproduce the high portion (near the peak) of the breakthrough curve in the first subreach (85 m) regardless of the functional form of the objective function. We attributed this to the presence of a large pool 35 m downstream of the injection location that caused segregation of solute flow which had been completely mixed across the stream upstream of the pool. The model was able to closely fit the breakthrough curves at $x=185$ and 323 m, most likely because the signature of the pool diminished downstream.

The parameters were well determined mathematically, as can be deduced from their small standard deviations. However, the fitting method did not always ensure that the parameter values represented the physical reality. For example, the flow rate in one experiment was found to be larger than in another, although the water level of the prior was lower. This could be due to a local optimum, in which case the problem could be alleviated using the approach Duan et al. (1994). Nevertheless, we believe that physical measurements should be made and incorporated into the parameter estimation procedure utilizing Bayesian estimation.

Our findings indicate that the representative values of parameters in a reach do not generally fall between the representative values of its subreaches. Hence, the expression ‘reach-averaged’ should be used cautiously. The lack of a reach-averaged value is rather unfortunate, because it is desirable from an engineering/science point of view to estimate the reach-scale parameters based on averages of the parameters in smaller scale experiments that can be better controlled.

We evaluated the practicality of using the TSM as a prediction tool. The results indicated that it is more reliable to extrapolate (going downstream) than to interpolate. We believe that this is due to two reasons. First, as one moves downstream from a subreach, the estimated parameter values lose the signature of the mechanisms occurring in the subreach. Eventually, if one is far downstream, one encounters the non-identifiability of parameters whereby many combinations of values provide essentially the same fit. Second, the values in each subreach were very different (Section 6.3), hence, the values estimated at the end of the reach were most likely ‘smoothed out’, and thus were not capable of representing the controls of the smaller scale. We also found that the OLS method provided the best estimate of parameter values for predicting the downstream breakthrough curves.

Acknowledgements

This study was supported in part by a grant from the United States Department of Agriculture (USDA), PENR-2003-01280. However, no official endorsement should be inferred. The authors are grateful to Ms. Kristina Culp from the Department of Civil and Environmental Engineering at Temple University for editing and improving the writing of the manuscript.

References

- Bard, Y., 1974. *Nonlinear Parameter Estimation*. Academic Press, San Diego, California.
- Bates, B.C., Townley, L.R., 1988. Nonlinear Discrete Flood Event Models. 2. Assessment of Statistical Nonlinearity. *Journal of Hydrology* 99, 77–89.
- Beck, J.V., Arnold, K.J., 1977. *Parameter Estimation in Engineering and Science*. Wiley, New York.
- Bencala, K.E., Walters, R.A., 1983. Simulation of solute transport in a mountain pool and riffle stream: a transient storage model. *Water Resources Research* 19 (3), 718–724.
- Boufadel, M.C., 1998. Unit hydrographs derived from the Nash model. *Journal of the American Water Resources Association* 34, 167–177.
- Boufadel, M.C., 2000. Estimation of the HEC1 loss parameters for routing the probable maximum flood. *Journal of the American Water Resources Association* 36 (1), 203–213.
- Boufadel, M.C., Suidan, M.T., Rauch, C.H., Venosa, A.D., Biswas, P., 1998. 2d variably saturated flows: physical scaling and bayesian estimation. *Journal of Hydrologic Engineering* 3, 223–231.
- Chapra, S.C., Runkel, R.L., 1999. Modeling impact of storage zones on stream dissolved oxygen. *Journal of Environmental Engineering, ASCE* 125 (5), 415–419.
- Choi, J., Harvey, J.W., 2000. Characterizing multiple timescales of stream and storage zone interaction that affect solute fate and transport in streams. *Water Resources Research* 36 (6), 1511–1518.
- Duan, Q.Y., Sorooshian, S., Gupta, V.K., 1994. Optimal use of the SCE-UA global optimization method for calibrating watershed models. *Journal of Hydrology* 3–4, 265–284.
- Fisher, H.B., List, E.J., Koh, R.C.Y., Imberger, J., Brooks, N.H., 1979. *Mixing in inland and coastal waters*. Academic Press. 479 pages.
- Gabriel, M., 2001. The role of geomorphology in the transport of conservative solutes in streams. Master thesis, Department of Civil and Environmental Engineering, Temple University, 78pages.
- Gabriel, M., Boufadel, M.C., 2002. Estimation of transient storage parameters from a stream tracer study, Hydrology Days, AWRA conference in Colorado.
- Gooseff, M.N., K, E., Bencala, D.T., Scott, R.L., 2005. Sensitivity analysis of conservative and reactive stream transient storage models applied to field data from multiple-reach experiments. *Advances in Water Resources* 28, 479–492.
- Harvey, J.W., Fuller, C.C., 1998. Effect of enhanced manganese oxidation in the hyporheic zone on basin scale geochemical mass balance. *Water Resources Research* 34 (4), 623–636.
- Harvey, J.W., Wagner, B.J., Bencala, K.E., 1996. Evaluating the reliability of the stream tracer approach to characterize stream-subsurface water exchange. *Water Resources Research* 32 (8), 2441–2451.
- HEC-HMS, US Army Corps of Engineer, 2001, Hydrologic modeling system HEC-HMS–User’s manual, 188 p.
- Jackman, A.P., Walters, R.A., Kennedy, V.C., 1984. Transport and concentration controls for chorine, strontium, potassium and lead in Uvas Creek, a small cobble-bed stream in Santa Clara County, California, USA, 2, Mathematical model. *Journal of Hydrology* 75, 111–141.
- Jones, B.J., Mulholland, P.J., 2000. *Stream and Groundwater*. Academic, San Diego, California.
- Kuczera, G., 1990. Estimation of runoff-routing model parameters using incompatible storm data. *Journal of Hydrology* 114, 47–60.

- Lane, S.N., Hardy, R.J., Elliott, L., Ingham, D.B., 2004. Numerical Modeling of Flow Processes Over Gravelly Surfaces Using Structured Grids And A Numerical Porosity Treatment. *Water Resources Research* 40 (1), W01302.
- Lasdon, L.S., Warren, A.D., Jain, A., Ratner M., 1979. A generalized reduced gradient algorithm, *ACM, Trans. Math. Software*, 4,34–50.
- Lasdon, L.S., Warren, A.D., 1980. GRG2's user's guide, Rep. Dept. of General Business. University of Texas, Austin, Texas.
- Levenspiel, O., 1999. *Chemical Reaction Engineering*, Third ed. Wiley. 668 p..
- Nordin, C.F., Troutman, B.M., 1980. Longitudinal dispersion in rivers: the persistence of skewness in observed data. *Water Resources Research* 16 (1), 123–128.
- Runkel, R.L., 1998. One-dimensional transport with inflow and storage (OTIS): a solute transport model for streams and rivers, U.S. Geological Survey Water Resources Investigations Report, 98–4018, 73.
- Rutherford, J.C., 1994. *River Mixing*, John Wiley, New York, 347 pp.
- Stream Solute Workshop, 1990. Concepts and methods for assessing solute dynamics in stream ecosystem. *Journal of the North American Benthological Society* 9 (2), 95–119.
- Thackston, E.L., Schnelle, Karl B., 1970. Predicting effects of dead zones on stream mixing. *Journal of the sanitary engineering division, Proceedings of The American Society of Civil Engineering SA2*, 319–331.
- Unver, O., Mays, L.W., 1984. Optimal determination of loss rate function and unit hydrographs. *Water Resources Research* 20, 203–214.
- Valentine, E.M., Wood, I.R., 1977. Longitudinal dispersion with dead zones. *Journal of the Hydraulics Division, ASCE*, 975–991.
- Harvey, J.W., Wagner, B.J., 2000. Quantifying hydrologic interactions between streams and their subsurface hyporeheic zones. In: Jones, J.B., Mulholland, P.J. (Eds.), *Streams and Ground Waters*. Academic Press, pp. 3–44.